Response of Open Cell Aluminum Foams to Fully Reversed Cyclic Loading

Hernan Pinto[1]; Sanjay R. Arwade[2]; and Patrick Veale[3]

Abstract: The response of metal foams to fully reversed cyclic loading has been investigated much less than the response to tension-tension and compression-compression cyclic loads. This paper describes tests of open cell aluminum foams that are subjected to fully reversed cyclic loading. Three different damage measures are evaluated as candidates for tracking the damage state in the material. These measures and associated failure criteria track the peak tensile stress, the peak compressive stress, and the ratio of the prepeak tensile and compressive material stiffnesses in each cycle. The peak tensile stress measure and criterion gave the most stable results. Finally, the fatigue lifetime is modeled by using a statistical Weibull model. **DOI: 10.1061/(ASCE)EM.1943-7889.0000298.** *© 2011 American Society of Civil Engineers.*

CE Database subject headings: Metals (material); Foam; Fatigue; Probability; Cyclic loads.

Author keywords: Metal foams; Fatigue; Probabilistic modeling; Weibull.

Introduction and Motivation

In the last few years, many writers have reported experimental and numerical results describing the mechanical properties of metal foams (McCullough et al. 2000; Sugimura et al. 1999; Ashby et al. 2000; Gibson and Ashby 1997; Gong and Jang 2005; Jang and Kyriakides 2008). In the domain of cyclic response, all such efforts have been focused on uniaxial tension-tension (TT) and compression-compression (CC) loading in which the sign of the maximum principle stress does not change during loading. As a result of this previous research, extensive knowledge of fatigue failure mechanisms in metal foams has been developed (McCullough et al. 2000; Sugimura et al. 1999; Harte et al. 1999). Until now, however, only a single paper, which considered closed cell aluminum foams, has been published that addresses the response of metal foams to cyclic loading that is fully reversed—that is, in which the load cycles are symmetric with a zero mean load or zero mean strain (Ingraham et al. 2009). The present study seeks to populate the final remaining gap in the open literature describing the fatigue response of aluminum foams, corresponding to the fully reversed cyclic loading of open cell aluminum foams. Once the description of the fatigue response under a wide variety of loading conditions is completed, designers hopefully may more fully explore the design space of possible applications of metal foams.

A similar qualitative response has been observed for the cyclic response of metal foams to TT and CC loading (McCullough et al. 2000; Sugimura et al. 1999; Ashby et al. 2000; Gibson and Ashby, 1997). For TT loading, the specimen progressively elongates during load cycling until the material sample separates into two pieces; for CC loading the specimen progressively shortens, eventually accumulating large permanent strains on the order of 50%. Under TT loading, material separation occurs at approximately 1% accumulated tensile strain for low density foams, and under CC loading the useful life of the material ends when the accumulated compressive strain reaches approximately 2% for low density foams. This value of the accumulated compressive strain corresponds to the point in the deformation history at which the rate of permanent strain accumulation accelerates rapidly.

In this paper, the writers report the results of experiments conducted to characterize the response of aluminum open cell foams to fully reversed cyclic loading. Under symmetric, strain-controlled cyclic loading, permanent strains cannot, by definition, develop. Three measures were therefore investigated for quantifying the damage state in the material and defining a point in the load-deformation history at which the material sample can be said to have failed, meaning that its useful life in an engineering application has been exhausted. These measures involve the peak compressive and tensile stresses achieved in each load cycle, and the ratio of the prepeak stiffness in the tension and compression parts of the load cycle. This third measure is the one suggested by Ingraham et al. (2009). The three damage measures are called hereafter the peak compressive stress, peak tensile stress, and stiffness ratio measures. Associated with each of these measures is a threshold value that defines the fatigue failure criterion.

In addition to the relative merits of the three damage measures and failure criteria for open cell aluminum foams subjected to symmetric cyclic loading, the results of the fatigue experiments are presented in the form of curves showing the damage evolution corresponding to each of the damage measures. On the basis of these data, the full $\varepsilon - N$ field is obtained by using a statistical Weibull fatigue analysis model (Castillo et al. 2007, 2008; Castillo and Fernndez-Canteli 2001; Pinto 2009). This statistical model is adopted in lieu of the traditional determinstic models such as the Basquin appoach (Basquin 1910), the Coffin-Manson approach (Coffin 1954; Manson 1965) and Morrow's model (Morrow 1964, 1965). The statistical Weibull model possesses

[1]Escuela de Ingeniería en Construcción, Pontificia Universidad Católica de Valparaíso, Chile. E-mail: hernan.pinto@ucv.cl

[2]Assistant Professor, Dept. of Civil and Environmental Engineering, Univ. of Massachusetts, Amherst, MA 01003 (corresponding author). E-mail: arwade@ecs.umass.edu

[3]Formerly, graduate student, Dept. of Civil and Environmental Engineering, Univ. of Massachusetts, Amherst, MA 01003.

Note. This manuscript was submitted on November 24, 2010; approved on July 1, 2011; published online on November 15, 2011. Discussion period open until May 1, 2012; separate discussions must be submitted for individual papers. This paper is part of the ***Journal of Engineering Mechanics***, Vol. 137, No. 12, December 1, 2011. ©ASCE, ISSN 0733-9399/2011/12-911–918/$25.00.

two distinct advantages over established deterministic approaches: (1) the total strain amplitude can be introduced in a straightforward way as the independent parameter of the strain-lifetime curves, replacing the plastic strain amplitude; and (2) a direct probabilistic description of the whole strain-lifetime field is obtained that arises from rigorous statistical and physical conditions, rather than from arbitrary assumptions. Nevertheless, the writers of this paper acknowledge that certain features of the mechanics of the cyclic deformation of metal foams are inconsistent with the assumptions of the Weibull model—namely, that metal foams are not brittle, defect-sensitive materials. Therefore, the writers propose that the Weibull model is not an explanation of the underlying mechanics, but essentially it is a phenomenological model for the strain-life relation that has the significant advantage of naturally incorporating a probabilistic treatment of the fatigue lifetime.

The paper contains sections that, sequentially: describe the material and the experimental procedure; define the damage measures and associated failure criteria for open cell aluminum foams subjected to symmetric cyclic loading; describe the results of the fatigue tests in terms of each of the damage measures and calibration of the statistical Weibull model to the results; contain a detailed discussion of the results obtained using each of the damage measures; and summarize the conclusions of the study and describe some possible avenues for future investigation.

Material and Experimental Procedure

This section describes the materials used in the fatigue tests and the experimental methods used to obtain the strain-lifetime curves for the open cell aluminum foam.

Material

The metal foam used in this study is commercially available under the name Duocel and is manufactured by ERG Aerospace of Oakland, California. The base metal of the foam is 6061 aluminum alloy. Two sets of foams were tested, one with 20 pores per inch (ppi) and an average relative density of 7.5% and one with 40 pores per inch and an average relative density of 7.38%. The specimens were machined to a dog bone shape with a test cross section of 25.4 mm wide by 50.8 mm thick (Fig. 1). The thickness of the specimens was a uniform 50.8 mm in the test and shoulder sections. The specimens were sized in accordance with the recommendation that the smallest specimen dimension should be no less than eight cell diameters in any dimension to avoid size and edge effects on the material response (Andrews et al. 2001).

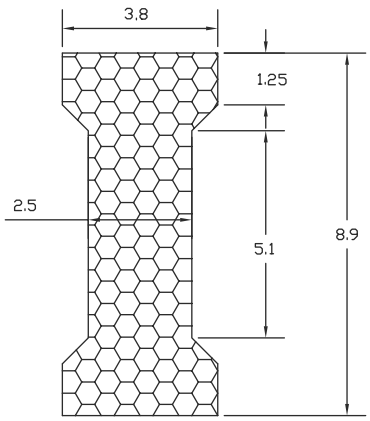

Fig. 1. Test specimen (dimensions are in cm)

Experimental Procedures

The experiments were conducted in an Instron testing machine under strain control at the Gunness Laboratory at the University of Massachusetts, Amherst. The test set up (Fig. 2), includes two grips machined from stainless steel, to which the specimen was attached with two-part epoxy, and an extensometer attached to the specimen with a gauge length equal to the length of the reduced section of the dog bone specimen. For each porosity, three specimens were tested at six different strain amplitudes (0.3%, 0.4%, 0.5%, 0.75%, 1.0%, 1.25%) with a constant frequency of 0.1 Hz. The extensometer readings, rather than the crosshead displacements, were used to calculate the strain used for test control. The specimens were adhesively bonded to the flat loading platens because of the difficulty of gripping low density foams by using standard mechanical grip fixtures. Adhesive bonding has also been used in successful fatigue tests of closed cell aluminum foams (Ingraham et al. 2009). The use of a constant cycling frequency results in variable strain rates being applied to the material. In these tests, the strain rate varied from 6×10^{-4} s^{-1} to 2.5×10^{-3} s^{-1}, which is a relatively narrow range. Ingraham et al. (2009) and Deshpande and Fleck (2000) have shown experimentally that such variations in the strain rate have a negligible effect on the mechanical response of aluminum foams. It has therefore been assumed that the effect of the strain rate variation present in the tests described here can be neglected.

Damage Measures and Failure Criteria

The number of cycles to failure is the key observation to be made during a fatigue test, and is the key parameter in designing against fatigue failure. Metal foams subjected to symmetric cyclic loading lose their engineering utility long before a single dominant crack appears and causes separation of the material specimen. It is therefore necessary to define failure criteria that can detect this loss of integrity that is not readily observed by the naked eye. Such failure criteria must be defined on the basis of damage measures or parameters that quantify the evolution of the damage state in the material. In this paper, the writers investigate three different damage measures and associated failure criteria; all were investigated on the basis of the principle that the stiffness of the material decreases during symmetric cyclic loading. The proposed measures are the

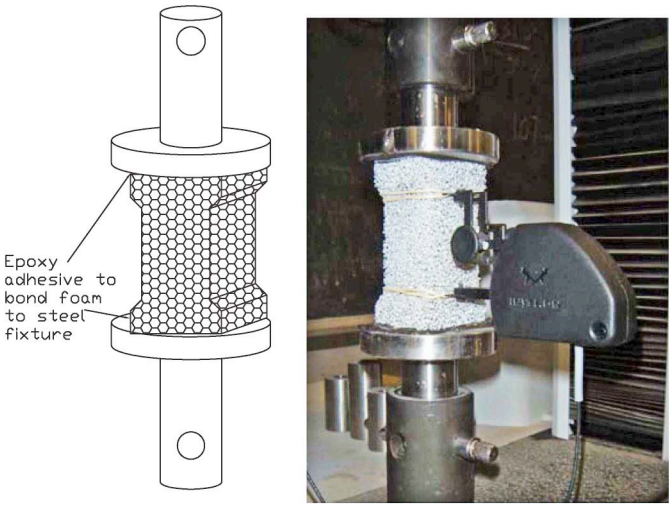

Fig. 2. Test specimen configuration (image by Hernan Pinto)

stiffness ratio, the peak tensile stress, and the peak compressive stress.

Stiffness Ratio Damage Measure

Ingraham et al. (2009) proposed the stiffness ratio damage measure for closed cell aluminum foams. It is the ratio of the prepeak compressive and prepeak tensile stiffnesses of the material

$$R_s = \frac{H_C}{H_T} \tag{1}$$

where H_{Cn} corresponds to the prepeak compressive stiffness and H_T is the prepeak tensile stiffness. The value of this damage measure at cycle n of the loading history is denoted by $R_{sn} = H_{Cn}/H_{Tn}$. The initial value R_{s0} in an undamaged material is 1, and the associated failure criterion has been established as

$$R_s = 1.5 \tag{2}$$

on the basis of empirical observations that the prepeak tensile stiffness tends to decrease with increasing fatigue cycles, whereas the prepeak compressive stiffness simultaneously increases, leading to an increase in R_s (Ingraham et al. 2009). By using this failure criterion, the number of cycles to failure, N_f, of the material is defined as

$$N_f = \min_n\{n\text{: } R_{sn} > 1.5\} \tag{3}$$

Fig. 3 shows that the prepeak tensile stiffness decreases with the number of cycles from a value H_{T0} for the first cycle to H_{Tn} for the nth cycle. On the other hand, the compressive prepeak stiffness increases from an initial value of H_{C0} for the first cycle to H_{Cn} for the nth cycle.

Peak Tensile Stress Damage Measure

The peak tensile stress damage measure is defined on the basis of the observation that, in a strain-controlled fatigue test, the peak tensile stress σ_T in each cycle tends to decrease as the material becomes more damaged (Fig. 4). The associated failure criterion is defined on the basis of a threshold value of the peak tensile stress such that, when the value of σ_T drops below this threshold, the material is assumed to have exhausted its engineering utility. The maximum tensile peak stress $\sigma_{T\,\max}$ will be recorded during one of the first loading cycles and serves as the reference value of σ_T. The limiting value of σ_T is of course $\sigma_T = 0$, which occurs

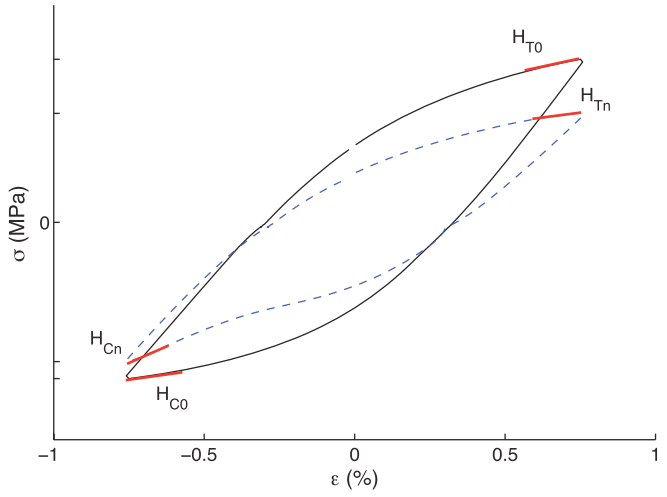

Fig. 3. Schematic H_c/H_t ratio change

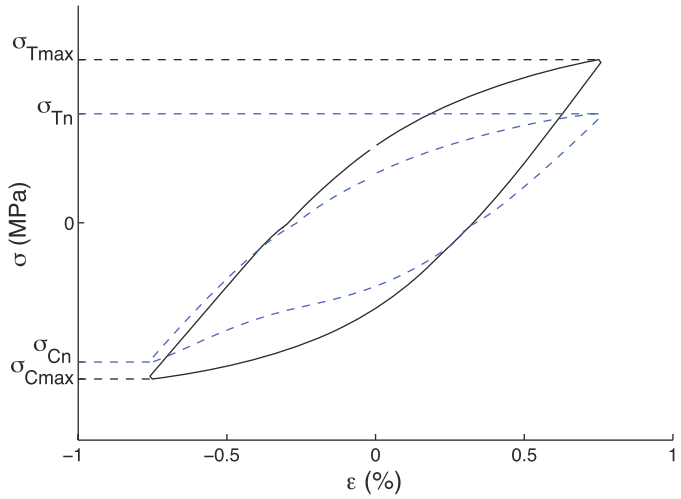

Fig. 4. Schematic drop in the tensile and compressive (in absolute value) peak stress during the application of the cyclic load

at material separation; however, as with the other damage measures, the material's integrity is lost well in advance of material separation. The notation σ_{Tn} indicates the peak tensile stress in cycle n of the loading history. The writers define the failure criterion associated with the $\sigma_{T\,\max}$ damage measure as

$$\sigma_T = 0.8\sigma_{T\,\max} \tag{4}$$

with the associated fatigue lifetime definition as

$$N_f = \min_n\{n\text{:}\sigma_{Tn} < 0.8\sigma_{T\,\max}\} \tag{5}$$

The choice of the threshold value is essentially arbitrary and can be tailored to a particular application, as needed.

Peak Compressive Stress Damage Measure

The peak compressive stress damage measure is similar to that of the peak tensile stress, but it instead considers the peak compressive stress, σ_C, in each loading cycle, and it establishes a failure criterion that is defined on the basis of the reduction of the peak compressive stress during cyclic loading. Fig. 4 shows that σ_C decreases during the application of cyclic loading from the maximum compressive stress ($\sigma_{C\,\max}$), which is established in the first few cycles of the loading history. Unlike the tensile stress damage measure, σ_C is not expected to approach zero with increasing fatigue loading, and the reduction of σ_C occurs more slowly than the reduction in σ_T. Therefore, the fatigue failure criterion, defined on the basis of the peak compressive stress damage measure, is established as

$$\sigma_C = 0.90\sigma_{C\,\max} \tag{6}$$

with an associated fatigue lifetime of

$$N_f = \min_n\{n\text{: } \sigma_{Cn} < 0.9\sigma_{T\,\max}\} \tag{7}$$

Experimental Results and Fatigue Modeling

This section contains a description of the results of the fatigue testing conducted on the open cell aluminum foams and the resulting statistical strain-lifetime curves.

Damage Evolution

During testing, the load and extensometer strain were recorded at a frequency of 10 Hz. From these data, the writers can identify the peak tensile and compressive stress in each cycle and can calculate the prepeak tensile and compressive stiffnesses. The prepeak stiffness are calculated by performing a linear regression on the upper and lower 5% of the stress-strain curve for the tensile and compressive parts of each loading cycle. In the test configuration, therefore, the damage measures are not tracked directly during testing; rather they are determined during the postprocessing of the experimental observations. Fig. 5 shows the damage evolution curves for each damage measure, each applied strain amplitude, and each foam porosity. The peak tensile and peak compressive stress damage measures are normalized by $\sigma_{T\,\max}$ and $\sigma_{C\,\max}$, respectively.

The stiffness ratio damage measure is not well behaved for applied strain amplitudes above 0.75%. This is shown in Figs. 5(a) and 5(b) in the dashed lines that drop rapidly below 0.5. The stiffness ratio damage measure essentially appears somewhat unstable for large deformation loading. Even for lower applied strain amplitudes [see the 0.40% curve in Fig. 5(a)], the stiffness ratio measure does not give a smooth damage accumulation curve, indicating occasional drops in the damage measure that are nonphysical.

The peak tensile and peak compressive stress damage measures give smooth damage accumulation curves for all applied strain amplitudes. Nevertheless, the peak tensile stress damage measure exhibits a more distinct acceleration of damage (evident as a rapid drop in the ratio $\sigma_T/\sigma_{T\,\max}$) that will, in general, make it easier to identify precisely the point at which the failure criterion is met. The damage accumulation curves that track the peak tensile stress measure show one unexpected feature in the results for the tests conducted at the applied strain amplitude of 0.30%—namely, a rising value of σ_T during approximately the first 500 cycles of testing. The writers have not identified a mechanism that is clearly responsible for this feature and have used the maximum value of the peak tensile stress, rather than the initial value, to establish the damage measure. This is another reason why it is not possible to directly track the damage evolution during testing: the value of $\sigma_{T\,\max}$ and $\sigma_{C\,\max}$ may not be known even after the first few cycles of testing.

The damage accumulation curves indicate that the stiffness ratio measure is less stable than the two stress-based measures, and that the peak tensile stress measure is somewhat preferable to the peak compressive stress measure. This discussion will be revisited in the context of the fatigue lifetimes calculated from the damage accumulation curves. Fig. 6 most clearly shows how the stiffness ratio measure fluctuates wildly for large amplitude loading and that it is

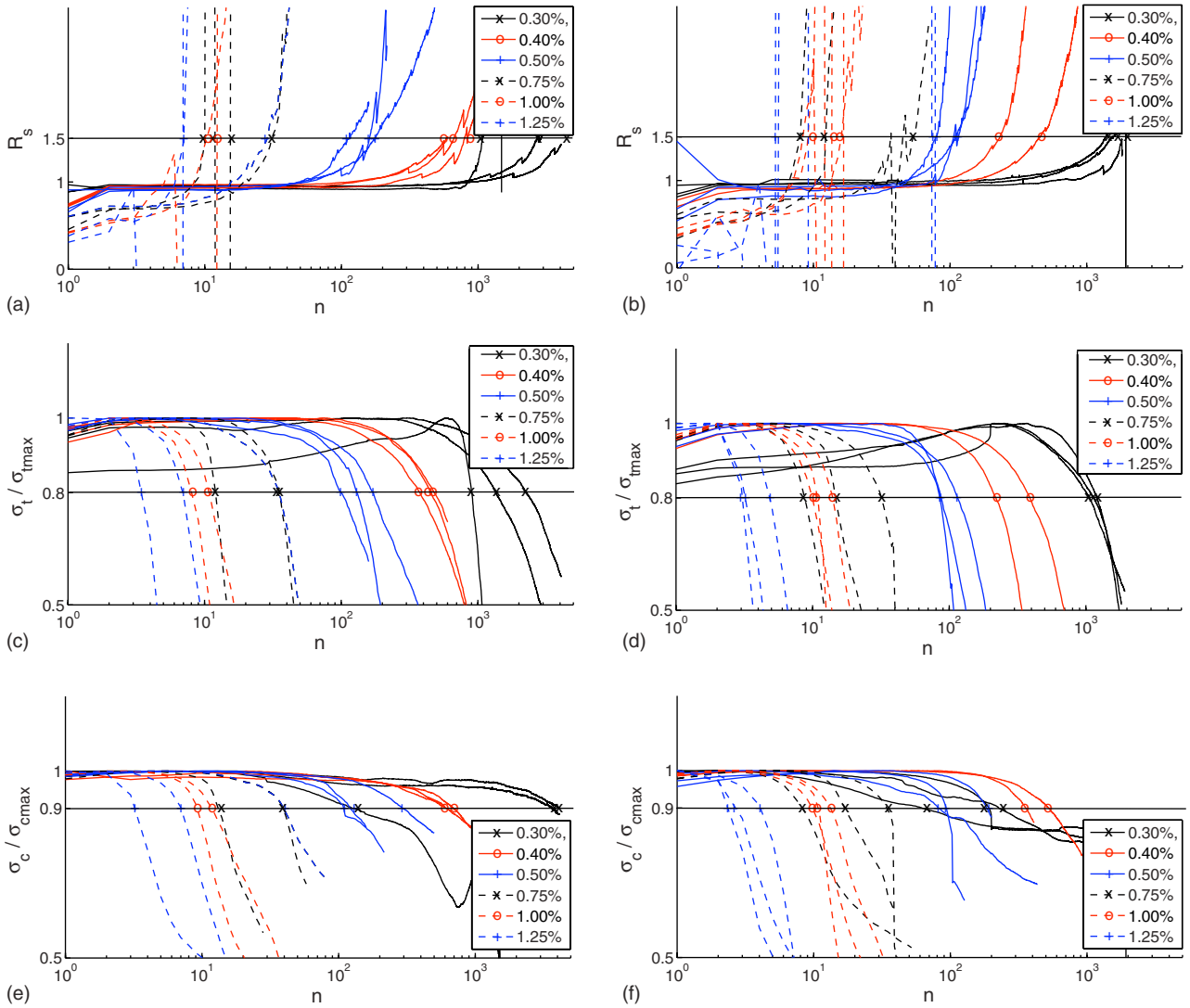

Fig. 5. Damage accumulation curves for each failure criteria and porosity: (a), (c), and (e) are for 20 ppi foam; (b), (d), and (f) are for 40 ppi foam

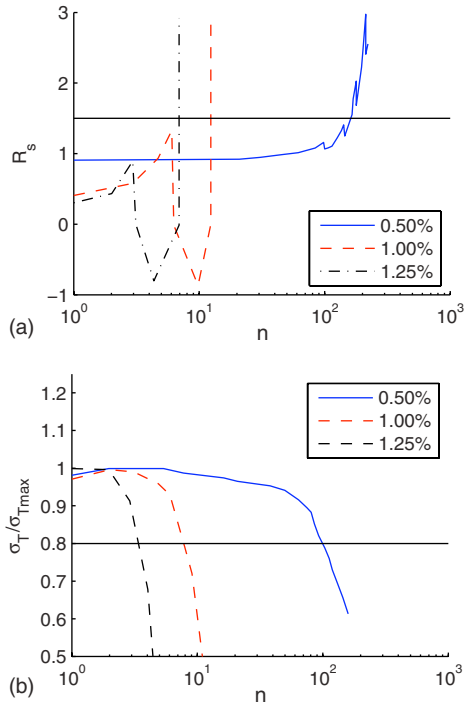

Fig. 6. Detail of three damage accumulation curves from Fig. 5: (a) is for 20 ppi foam; (b) is for 40 ppi foam

not even monotonic for moderate amplitude loading. The peak tensile stress criterion, on the other hand, evolved rather smoothly and essentially monotonically, even when the loading amplitude was large.

Fatigue Lifetimes

On the basis of the failure criteria defined in Eqs. (2), (4), and (6) and the definitions of the fatigue lifetimes given by Eqs. (3), (5), and (7), the fatigue lifetime for each of the test samples can be determined from the stress-strain records captured during the tests.

Table 1. Fatigue Test Parameters and Results for the 20 ppi Metal Foam

Specimen	Relative density (%)	ε_a (%)	$R_s > 1.5$	$\sigma_T < 0.8\sigma_{T\,\max}$	$\sigma_C < 0.9\sigma_{C\,\max}$
20-12	7.87	0.30	2,316	1,131	2,316
20-17	7.53	0.30	2,706	1,351	3,648
20-18	7.53	0.30	1,081	902	1,260
20-05	7.93	0.40	589	481	602
20-10	7.418	0.40	796	454	695
20-11	7.41	0.40	666	377	613
20-04	7.53	0.50	111	101	123
20-06	7.35	0.50	173	171	295
20-14	8.05	0.50	161	131	109
20-03	7.41	0.75	11	13	14
20-07	7.18	0.75	31	36	40
20-09	7.70	0.75	29	36	40
20-01	7.29	1.00	15	16	17
20-02	7.47	1.00	13	9	10
20-16	7.53	1.00	11	11	12
20-08	7.18	1.25	6	3	3
20-13	7.58	1.25	7	4	4
20-15	7.47	1.25	8	7	8

Table 2. Fatigue Test Parameters and Results for the 40 ppi Metal Foam

Specimen	Relative density (%)	ε_a (%)	$R_s > 1.5$	$\sigma_T < 0.8\sigma_{T\,\max}$	$\sigma_C < 0.9\sigma_{C\,\max}$
40-12	7.24	0.30	1,380	1,205	226
40-13	7.41	0.30	1,536	1,068	192
40-18	7.58	0.30	1,800	1,145	620
40-09	7.18	0.40	232	220	356
40-14	7.18	0.40	456	391	524
40-20	7.87	0.40	271	212	244
40-02	7.12	0.50	110	116	185
40-08	7.18	0.50	79	86	94
40-16	7.64	0.50	107	88	82
40-06	7.53	0.75	9	9	9
40-07	7.24	0.75	13	15	17
40-17	7.18	0.75	37	32	35
40-01	7.58	1.00	9	10	10
40-05	7.35	1.00	10	11	11
40-15	7.24	1.00	16	15	14
40-03	7.41	1.25	6	4	3
40-04	7.35	1.25	10	5	5
40-19	7.47	1.25	6	4	3

These results are presented in Tables 1 and 2 for the 20 and 40 ppi foams, respectively.

Fatigue Models

The experimental fatigue life results were placed in the framework of the statistical Weibull model [Eq. (8)] (Castillo et al. 2007, 2008; Castillo and Fernndez-Canteli 2001; Pinto 2009), which defines the cumulative distribution function of the strain-lifetime curves according to

$$F(\log N_f; \log \Delta\varepsilon_a) = 1 - \exp\left\{-\left(\frac{(\log N_f - B)(\log \Delta\varepsilon_a - C) - \lambda}{\delta}\right)^{\beta}\right\} \quad (8)$$

$$\log N_f \geq B + \frac{\lambda}{\log \Delta\varepsilon_a - C} \quad (9)$$

where $B = \log N_0$; $C = \log \varepsilon_{a0}$; and λ, δ, and β are the nondimensional model parameters with N_0 as the minimum fatigue lifetime and ε_{a0} as the fatigue limit.

The parameters are divided into two categories: the first containing the threshold parameters (B and C) and the second, the Weibull parameters (β, δ and λ). The writers followed the established two-stage parameter estimation procedure that entails, first, estimating the threshold parameters by using a constrained least-squares method and, second, estimating the Weibull parameters by using a maximum likelihood approach (Castillo et al. 2007, 2008; Castillo and Fernndez-Canteli 2001; Pinto 2009). Through the parameter estimation process, the set of model parameters in Tables 3 and 4 are obtained. The corresponding $\varepsilon - N$ fields is shown in Fig. 7.

Table 3. Weibull Parameters for the 20 ppi Metal Foam

Criterion	B	C	β	δ	λ
$R_s > 1.5$	−8.1083	−8.2192	20	16.2375	22.487
$\sigma_T < 0.8\sigma_{T\,\max}$	−22.3992	−11.6395	13.1924	23.4651	150.7185
$\sigma_C < 0.9\sigma_{C\,\max}$	−20.0156	−10.8017	20	37.8166	101.3195

Table 4. Weibull Parameters for the 40 ppi Metal Foam

Criterion	B	C	β	δ	λ
$R_s > 1.5$	−3.0469	−7.0799	7.1482	4.8794	8.8123
$\sigma_T < 0.8\sigma_{T\,\max}$	−8.5126	−8.4384	6.6686	6.7942	34.5434
$\sigma_C < 0.9\sigma_{C\,\max}$	−42.4668	−18.9089	11.5118	77.6863	564.6212

Discussion

Two of the three damage measures described here, the peak tensile and peak compressive stress measures, are trivially obtained from the load-deformation data recorded during the experiments because they correspond simply to the peak tensile and compressive loads in each cycle divided by the specimen cross sectional area. The stiffness ratio criterion requires some moderate postprocessing of the load-displacement data because the prepeak tensile and compressive stiffnesses must be calculated by making a linear regression of the loading parts of the hysteresis curve in the neighborhood of the peak.

An observation that can be made from Fig. 5 is that the stiffness ratio damage measure is unstable, particularly for low cycle fatigue induced by large applied strains. In some cases, the stiffness ratio even drops far below its initial value of 1.0, indicating that in some cycles the prepeak compressive stiffness was less than the prepeak tensile stiffness, which is an unexpected result. A possible explanation for this is that, at high applied strains, the damage state in the material is evolving so rapidly that the damage state changes substantially within a cycle—that is, between the tensile and compressive peaks. Because the prepeak tensile and compressive stiffnesses

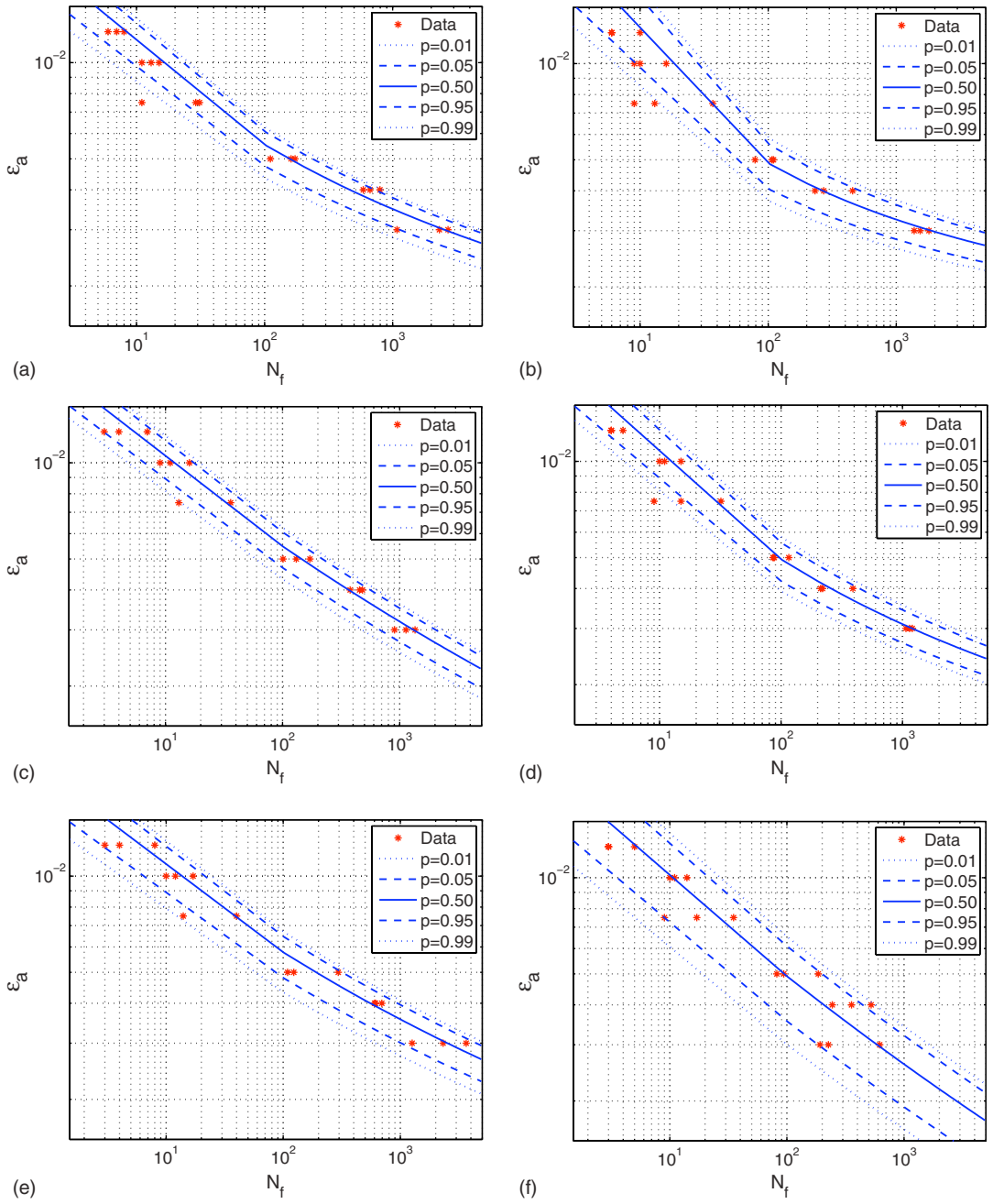

Fig. 7. $\varepsilon - N$ field curves for the 20 and 40 ppi metal foam for each one of the criteria proposed: (a), (c), and (e) are for 20 ppi foam; (b), (d), and (f) are for 40 ppi foam

are both decreasing during cyclic loading, the rapid damage evolution could lead to individual cycles in which the compressive stiffness exceeds the tensile stiffness. Furthermore, the stiffness ratio criterion depends on performing a linear regression on the last part of the tensile and compressive loading curves. This is a straightforward operation; however, the results can be sensitive to the portion of the loading curve that is included in the regression. This is especially true for the compressive loading curve in which a sharp increase occurs in stiffness when cracks that had been open under tensile loading close and increase the stiffness.

Both stress-based damage measures provide relatively smooth damage accumulation curves, and the rate of decay of the peak compressive stress is slower than that for the peak tensile stress. Thus, if one desires that the failure criteria give comparable fatigue lifetimes, the threshold value of the peak compressive stress should be set at a higher value than that for the peak tensile stress. In this study, these values are set at $0.9\sigma_{C\,\max}$ and $0.8\sigma_{T\,\max}$, respectively. The damage accumulation curves from the peak compressive stress measure display one undesirable characteristic: an inflection point that points to the possible presence of an asymptotic value of the peak compressive stress in the high cycle limit. This is shown, for example, in the 0.40% damage accumulation curve in Fig. 5(e) and the 0.50% curve in Fig. 5(f). Furthermore, the peak compressive stress failure criterion yields very low values of the fatigue lifetime for the 40 ppi foam with the applied strain amplitude of 0.30% (see Table 4). Examining the damage accumulation curves for these samples [see Fig. 5(f)] reveals that the peak compressive stress for these samples dropped after approximately 5×10^2 cycles but then stabilized until the end of the test at approximately 1×10^3 cycles. It is certainly preferable to have a damage measure that is monotonic once significant damage begins to accumulate in the material. The peak tensile stress criterion is preferable from this point of view.

Table 5 shows that the 40 ppi foams tend to show a lower fatigue lifetime than the 20 ppi foams. A possible explanation of this phenomenon is that the stress state (i.e., the balance among the axial, bending, and shearing stresses) in the ligaments differs for the 20 and 40 ppi foams. The writers do not propose a precise mechanism for this feature of the response at this point, but are conducting numerical investigations into the influence of pore size on ligament stress state as part of a follow-up study to this work. The writers did not measure inhomogeneities in the strain field that may arise during cyclic loading; however, the samples were visually inspected, following their removal from the testing apparatus. Crush bands and macroscopic cracks that have been reported in previous studies were not observed; in fact, the material appeared, to the naked eye, undamaged. Because crush bands and macroscopic cracks have been observed in all previous studies of the cyclic response of metal foams, the writers do not propose that the mechanism of damage in our the specimens differs, but that the crush bands and cracks remained unobserved because the testing was stopped while substantial residual strength remained in the specimens. A finding, therefore, of this study is that substantial degradation of material strength can occur before macroscopic damage is present.

Table 5. Fatigue Test Parameters and Results for the 40 ppi Metal Foam

$\varepsilon_a(\%)$	Criterion	20 ppi	40 ppi	Reduction of N_f for the 40 ppi (%)
0.30	R_s	2,034	1,572	23
	σ_T	1,128	1,139	0
	σ_C	2,408	346	86
0.40	R_s	683	319	53
	σ_T	437	274	37
	σ_C	636	374	41
0.50	R_s	148	98	34
	σ_T	134	96	28
	σ_C	175	120	31
0.75	R_s	23	19	17
	σ_T	28	18	36
	σ_C	31	20	35
1.00	R_s	13	11	15
	σ_T	12	12	0
	σ_C	13	11	15
1.25	R_s	7	7	0
	σ_T	4	4	0
	σ_C	5	3	40

For each failure criterion, a statistical Weibull model for the fatigue lifetime has been calibrated, providing directly the cumulative distribution functions for the fatigue lifetime at a specified porosity and applied strain amplitude. At this point, it is appropriate to address the question of why the low cycle fatigue life of metal foams may be important to engineers because metal foams have traditionally been deployed only in situations in which the loading will be monotonic compression or cyclic at low stress or strain amplitudes. Moradi (2011) shows that composite members composed of a thin-walled tube and a metal foam core have a superior buckling and postbuckling response and increased energy dissipation under monotonic loading. It is a plausible extension of that result that such an energy-dissipating postbuckling response could be used to great advantage. For example, it could be used to ameliorate the seismic response of structures framed from thin-walled members, such as cold-formed steel sections. The key to this behavior, however, is that the foam must maintain its structural integrity through a relatively low number of high amplitude cycles. For applied strain amplitudes that lead to fatigue life on the order of 10^3 cycles, the applications are admittedly harder to define at this time and the writers hope that publication of this data may inspire design engineers to consider a broader design space for the material.

An exhaustive comparison of the results presented here and those previously reported for closed cell aluminum foams (Ingraham et al. 2009) is not possible because of the different strain amplitudes used; however, both studies performed tests at an applied strain amplitude of 0.50%. The closed cell foams showed a mean fatigue life of 68 cycles at a relative density of 8.7%, whereas the open cell foams showed a mean fatigue life of 148 cycles at a relative density of 7.6% with 20 ppi and 98 cycles at a relative density of 7.3% with 40 ppi. This preliminary indication therefore is that open cell foams, at approximately the same relative density, exhibit a longer fatigue life than closed cell foams at a comparable density. This phenomenon remains to be confirmed by a more extensive set of comparable tests; however, a possible explanation is that, for the same relative density, the open cell foams concentrate the material in somewhat stockier ligaments than do the very thin faces of the closed cell foam.

A direct comparison with published investigations of the CC and TT fatigue behaviors reported in the literature (Sugimura et al. 1999; Harte et al. 1999; McCullough et al. 2000) is challenging because each of these studies used stress-controlled fatigue cycling and different failure criteria. For the TT tests, failure occurred when the specimen separated into two parts; for the CC tests, failure occurred either when the accumulated ratcheting compressive strain reached a value comparable to the yield strain or when a noticeable acceleration appeared in the accumulation of the ratcheting strain. In the tests described here, the ratcheting strain could not accumulate because of the strain-controlled nature of the tests.

Nevertheless, the following is a brief description of the TT and CC context in which the present results should be placed. Harte et al. (1999) found that—at an R ratio of 0.1 and a maximum tensile and compressive stress of 0.7 to 1.4 times the yield stress—the fatigue lifetimes ranged from 10^2 to 10^7 cycles, and the fatigue life was essentially identical in tension and compression. Sugimura et al. (1999) found that, with $R = 0.1$, when the maximum compressive stress (the tests were only performed in the CC mode) ranged from 0.7 to 0.9 times the yield stress, the fatigue lifetime ranged from 10^2 to 10^6 cycles. Finally, McCullough et al. (2000) found that, for maximum stress values of 0.5 to 1.1 times the yield stress, the fatigue life ranged from 10^3 to 10^8 cycles. This study was the only one to find a significant difference between the TT and CC behavior. The present tests used $R = -1$ (defined by strain rather than by the stress), and applied strain values of 1.1 to 5 times the yield strain. Fatigue lifetimes were found to vary from 10^0 to 10^3 cycles. The low amplitude, long lifetime end of this range closely coincides with loading that is near the yield strain. In the published CC and TT literature, stress-controlled tests with $R = 0.1$ and maximum applied stress near the yield stress, gave lifetimes of approximately 10^2 to 10^4 cycles. These are within the order of magnitude of what the present tests revealed for a strain-controlled loading of amplitude near the yield stress. Given the substantial differences in the testing protocols followed in the published TT and CC investigations and the present tests, no substantial evidence shows that the relationship between the loading amplitude and the fatigue lifetime is substantially different for reversed loading than for CC or TT loading.

Conclusion and Future Work

Three damage measures and associated failure criteria have been proposed for open cell aluminum foam subjected to strain-controlled cyclic loading symmetric with the zero strain. The damage measures correspond to the peak stress in tension and compression, and to the ratio of prepeak compressive and tensile stiffness (Ingraham et al. 2009).

These damage measures and failure criteria have been applied to a set of experiments conducted on open cell aluminum foams at applied strain amplitudes ranging from 0.003 to 0.0125. The results show that the stiffness ratio measure provides a good characterization of the damage accumulation at moderate to low loading amplitudes, but is somewhat unstable for the characterization of very low cycle fatigue. The peak compressive and peak tensile stress damage measures present stable damage accumulation curves across the range of applied strain amplitudes; however, the peak tensile stress measure accelerated more distinctly at the onset of material failure, rendering this measure as the most preferred of the three damage measures investigated here. The peak tensile stress damage measure also has the advantage of being easily calculated from the load-displacement records generated by fatigue testing.

The statistical Weibull model has been calibrated to the fatigue lifetimes estimated by using each of the damage measures and failure criteria. This model represents a direct statistical consideration of the fatigue behavior of the metal foam and it considers the total strain amplitude as the independent parameter instead of the plastic strain component.

The results presented here represent a characterization of the fatigue response of open cell metal foams to cyclic loading with load reversal. Such characterization is important for expanding the range of engineering applications in which metal foams are applied. Further investigation is needed to quantify the effect of the loading R ratio and to extend this characterization presented here into the domain of lower applied strain amplitudes and longer fatigue lifetime.

Acknowledgments

The writers of this paper are indebted to Mr. Robert Brack for his continuing support of the CEE department of the University of Massachusetts Amherst, and especially of research activities in the structural engineering and mechanics group. This work has also been partially supported by the United States National Science Foundation through grant #CMMI-1000334.

References

Andrews, E., Gioux, G., Onck, P., and Gibson, L. (2001). "Size effects in ductile cellular solids. Part II: Experimental results." *Int. J. Mech. Sci.*, 43, 701–713.

Ashby, M., Evans, A., Fleck, N., Gibson, L., Hutchinson, J., and Wadley, H. (2000). *Metal Foams: A Design Guide*, Butterworth-Heinemann, Woburn, MA.

Basquin, O. (1910). "The exponential law of endurance tests." *American Society Test Materials Proc., ASTM*, 10, 625–630.

Castillo, E., and Fernández-Canteli, A. (2001). "A general regression model for lifetime evaluation and prediction." *Int. J. Fract.*, 107, 117–137.

Castillo, E., Fernández-Canteli, A., Hadi, A., and López-Aenlle, M. (2007). "A fatigue model with local sensitivity analysis." *Fatigue Fract. Eng. Mater. Struct.*, 30, 149–168.

Castillo, E., Fernández-Canteli, A., Pinto, H., and López-Aenlle, M. (2008). "A general regression model for statistical analysis of strain life data." *Mater. Lett.*, 62, 3639–3642.

Coffin, L. (1954). "A study of the effect of cyclic thermal stresses on a ductile materials." *Trans. ASME*, 76, 931–950.

Deshpande, V. S., and Fleck, N. A. (2000). "High strain rate compressive behavior of aluminum foams." *Int. J. Impact Eng.*, 24, 277–298.

Gibson, L., and Ashby, M. (1997). *Cellular Solids*, 2nd Ed., Cambridge University Press, Cambridge.

Gong, L.K. S., and Jang, W. (2005). "Compressive response of open cell foams. Part I: Morphology and elastic properties." *Int. J. Solids Struct.*, 42, 1355–1379.

Harte, A., Fleck, N., and Ashby, M. F. (1999). "Fatigue failure of an open cell and closed cell aluminium alloy foam." *Acta Mater.*, 47, 2511–2524.

Ingraham, M., DeMaria, C., Issen, K., and Morrison, D. (2009). "Low cycle fatigue of aluminum foam." *Mater. Sci. Eng. A*, 504, 150–156.

Jang, W., Kraynik, A. M., and Kyriakides, S. (2008). "On the microstructure of open cell foams and its effect in elastic properties." *Int. J. Solids Struct.*, 45, 1845–1875.

Manson, S. (1965). "Fatigue: a complex subject-some simple approximation." *Exp. Mech.*, 5, 193–226.

McCullough, K., Fleck, N., and Ashby, M. (2000). "The stress-life fatigue behaviour of aluminium alloy foams." *Fatigue Fract. Eng. Mater. Struct.*, 23, 199–208.

Moradi, M. (2011). "Structural applications of metal foams considering material and geometrical uncertainty." Ph.D. thesis, University of Massachusetts, Amherst.

Morrow, J. (1964). "Fatigue Properties of Metals." *Fatigue Design Handbook Experimental Mechanics*, AE-4, Society for Automotive Engineers, Warrendale, PA.

Morrow, J. (1965). "Cyclic plastic strain energy and fatigue of metals. Internal friction, damping and cyclic plasticity." *ASTM Bull.*, 1965, 45–86.

Pinto, H. (2009). "Models for crack propagation and fatigue analysis based on strain and stress life data. applications." Ph.D. thesis, University of Cantabria, Santander, Spain.

Sugimura, Y., Rabiei, A., Evans, A. G., Harte, A. M., and Fleck, N. A. (1999). "Compression fatigue of a cellular Al alloy." *Mater. Sci. Eng. A*, 269, 38–48.